Enabling High Performance Green Propulsion for SmallSats

Robert K. Masse, Ronald A. Spores, May Allen, Scott Kimbrel
Aerojet Rocketdyne
11411 139th Pl N.E., Redmond, WA, 98052; 425-885-5000
robert.masse@rocket.com

Chris McLean
Ball Aerospace and Technologies Corporation
1600 Commerce Street, Boulder, Co, 80301; 303-939-6100
cmclean@ball.com

ABSTRACT

The inherent handling safety of green propellants is particularly facilitating for smallsats. Commonly manifested as one among a number of auxiliary payloads, simplicity of smallsat pre-launch operations is critical to maintaining a practical launch campaign. Moreover, trades have continually shown the increased density-specific impulse potentially offered by advanced propellants is enabling for a significant class of microsatellite missions (e.g. ESPA) where volumetric constraints preclude the use of conventional propellants such as hydrazine. The culmination of over two decades of research and development, NASA's Green Propellant Infusion Mission has recently completed hot-fire testing of prototype flight-design 1 N and 22 N green monopropellant thrusters operating on and AFRL-developed green propellant known as AF M315E. Scheduled for an inaugural on-orbit demonstration aboard an ESPA-launched microsatellite bus mid-2016, the GPIM thrusters and propulsion system represent the first flight-ready low-toxicity alternative to comparable hydrazine technologies, providing similar flexibility to operate at any duty cycle while delivering 50% greater density-specific impulse.

NOMENCLATURE

AFRL	=	Air Force Research Laboratory
APTL	=	Advanced Propellants Test Lab
EELV	=	Evolved Expendable Launch Vehicle
ESPA	=	EELV Secondary Payload Adapter
GPIM	=	Green Propellant Infusion Mission
GRAIL	=	Gravity Recovery and Interior Laboratory
HAN	=	Hydroxylammonium Nitrate
I_{sp}	=	Specific Impulse
ρI_{sp}	=	Density-Specific Impulse
MPE	=	Maximum Mission Projected Envelope
MRO	=	Mars Reconnaissance Orbiter
MSL	=	Mars Science Laboratory
NASA	=	National Aeronautics and Space Administration
PIP	=	Payload Interface Plate
SCAPE	=	Self-Contained Atmospheric Protection Ensemble

INTRODUCTION

The NASA Space Technology Mission Directorate (STMD) has initiated the Green Propellant Infusion Mission (GPIM) program with the objective of achieving the first on-orbit demonstration of a complete high-performance green propellant propulsion system by the end of 2016. Hosted on a Ball Aerospace BCP-100 ESPA-class spacecraft bus, the GPIM Technology Demonstration Mission (TDM) will employ an Aerojet Rocketdyne-developed advanced green monopropellant payload module as the sole means of on-board propulsion, performing a comprehensive battery of performance characterization and capabilities assessment maneuvers[1,2,3,4,5,6]. Whereas the ease of handling, and enhanced capabilities offered by green technologies offer broad benefits across the spectrum of missions currently performed by conventional hydrazine monopropellant technologies, for near-term infusion smallsat missions stand out as likely to play a leading role in two key respects.

Firstly, the potential advantages offered by advanced green propellants are particularly apposite to the needs of smallsats. Commonly launched as secondary payloads, minimal introduction of added safety-related logistics is paramount to minimized impact to the primary payload launch campaign. Further, trade studies have repeatedly shown the relative benefits offered by higher impulse density monopropellants are maximized for volume-limited systems, essentially the very definition of a smallsats in the context of in-space applications. In many cases, the higher density-specific impulse (ρI_{sp}) offered by advanced green propellants is

mission enabling, extending the capability of smallsats to perform missions that would ordinarily necessitate the use of larger and significantly more costly spacecraft. As a second consideration, the typically lower cost and shorter spans of smallsat missions make them ideal for first deployment of lower-heritage technologies than ventures where the potential loss of high vehicle and deployment investment costs, as well as revenues, are staked on mission success (e.g. geocommunications).

AF-M315E ADVANCED GREEN MONOPROPELLANT

The GPIM demonstration will employ a high-performance green propellant invented at the AFRL in 1998 known as AF-M315E, a true ionic liquid derived of hydroxylammonium nitrate (HAN), water, and an also highly hygroscope fuel (vs. other propellant formulations that actually include non-ionic, and in some cases toxic, volatiles such as methanol) [7]. Delivering approximately 50% higher ρI_{sp} than hydrazine (5% higher I_{sp} combined with a 46% higher density, AF-M315E offers comparable performance to traditional storable bipropellants for low ΔV missions while employing roughly half the number of components, thereby retaining the well-established increased reliability and reduced cost of traditional monopropellants. Many design issues and failure modes associated with long-duration interplanetary missions (e.g. control of mixture ratio, of propellant vapor diffusion and reaction, oxidizer flow decay) do not apply to an equally capable AF-M315E system.

AF-M315E (shown as routinely handled in Figure 1) derives its low-toxicity-hazard characteristics and high mixture stability (even to very low temperatures) from the high solubility and negligible vapor pressure of all solution constituents, such that indefinite exposure to the open environment poses no safety issue. As such,

Figure 1: AF-M315E propellant can be safely handled in open containers without need of respiratory protective equipment

AF-M315E simplifies the safe design and development of propulsion systems compared to conventional toxic propellants such as hydrazine. Since leakage of AF-M315E has been verified as a critical rather than catastrophic failure with range safety personnel per AFSPCMAN 91-710, only single-fault-tolerance is required for safety in handling flight systems. This alone accounts for significant savings, as redundant components are eliminated, yielding simpler architectures. Further, simpler and much less expensive design and verification criteria govern flight-qualification of fracture-critical hardware (e.g., propellant tanks) for non-hazardous propellants such as AF-M315E compared to hydrazine. The aggregate potential impact of these and increased performance-related cost savings is highly mission-dependent, but has been evaluated to tens of millions of dollars for large space missions such as Juno, MSL, and Europa; and to several million for more modest missions such as GRAIL and MRO[8].

With its ultra-low minimum storage temperature, AF-M315E yields an additional advantage mitigating operational concerns related to long-duration system thermal management. Whereas hydrazine space tanks and lines must be heated at all times to prevent freezing, AF-M315E cannot freeze (it undergoes glass transition at -80 ºC). Thus, during long coast periods an AF-M315E propulsion system may be allowed to fall to very low temperatures and later reheated for operation without risk of line rupture by phase-change-induced expansion. This can be particularly beneficial with respect to the often limited power budgets of smallsats, as well as interplanetary spacecraft and planetary ascent vehicles, which missions can call for years of propellant storage in cold environments. For <1 AU interplanetary exploration missions, solar power is naturally more limited than for Earth-orbiting satellites; e.g., equivalent solar power generation designs in Mars (e.g., MRO), Vesta (e.g., Dawn), and Jupiter (e.g., JUNO) orbits produce roughly 43%, 16%, and 3.7% of the electrical power they yield in Earth orbit, respectively. Tests also have demonstrated AF-M315E to have a significantly reduced sensitivity to adiabatic compression than hydrazine and other green propellants.

The cost savings green propellants promise through simplified range operations are quantifiable. The average contractual cost to load a NASA mission with conventional propellants is $135,000[8]. The cost for loading with AF-M315E will be a small fraction of this, and the associated schedule significantly expedited. Per current conventions, propellant loading operations require one shift for setup in SCAPE, a second shift waiting for propellant test confirmations, a third shift or

more for actual loading, and a final additional shift to break down the setup, during which all remaining launch processing staff must wait at costs exceeding $100k/day for a typical Class B NASA mission. Thus elimination of the interruption of launch processing associated toxic propellant loading can save more than $100k per launch and two shifts of schedule. Naturally, it follows that simplified range operations would equally benefit commercial users through lower launch costs. An early Aerojet Rocketdyne study evaluating replacement of hydrazine with a HAN-based advanced monopropellant for the Centaur reaction control system on the Atlas launch vehicle concluded ground support costs of fueling could be reduced by two-thirds[9].

GPIM PROPULSION SYSTEM OVERVIEW

Under development as a self-contained module to allow independent assembly at Aerojet Rocketdyne for high-level integration with the BCP-100 bus, the GPIM demonstration payload configuration, illustrated in Figure 2 and shown in schematic in Figure 3, bears high similarity to a traditional hydrazine system. Designed to integrate with the host spacecraft via its standard payload interface plate (PIP), the GPIM demonstration payload comprises a simple, single-string, blow-down AF-M315E advanced green monopropellant propulsion system employing five Aerojet Rocketdyne GR-1 1-N class thrusters, configured as a single primary divert thruster centered on an upper deck topping the payload's box-like primary structure flanked by four attitude-control thrusters mounted one each at the adjacent corners. (Whereas both 20-N and 1-N thrusters have been developed on the program for intended respective use for divert and attitude control; in response to delays in flight-readiness of the larger thruster, 1-N thrusters will be installed at all locations.) Because the AF-M315E propellant exhibits good compatibility with standard 6Al-4V titanium, propellant feed system components were able to be selected from a subset of heritage hydrazine system components that are compatible with little or no modification. (AF-M315E is not compatible with iron-bearing metals for long-duration storage.) Likewise, the GPIM demonstration payload module employs a conventional ATK model 80581 hydrazine propellant tank positioned near its center, all materials of construction of which have been successfully verified in thermally accelerated aging tests to be compatible with AF-M315E for durations of up to at least two years.

Aside from the 50% increased impulse delivered at comparable system volume, mission design-related distinctions between the GPIM and a traditional hydrazine system relate principally to differences in the thermal characteristics of AF-M315E vs. conventional thrusters. Due to the advanced monopropellant thrusters' elevated minimum start temperature, catalyst bed preheat power requirements are higher than a typical hydrazine system. This increase is partially offset, however, by savings associated with the thrusters' single (instead of conventional dual) seat valves, as well as much reduced required power for system thermal management during non-operating periods facilitated by the propellant's demonstrated storability at very low temperatures. Radiation and conduction from the advanced monopropellant thrusters' high temperature chambers also impart a moderate increase in the thermal load to the system mounting interface.

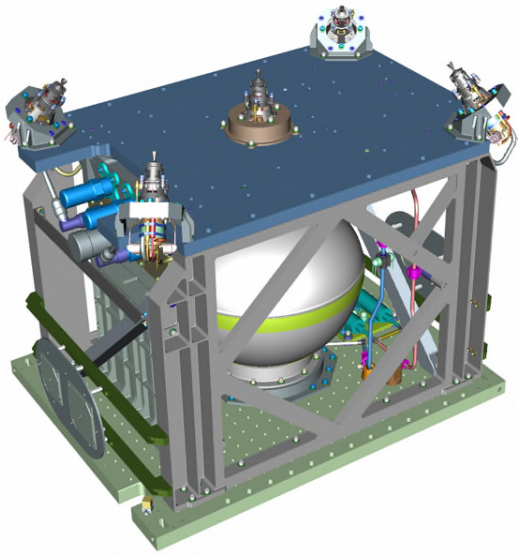

Figure 2: AF-M315E Propulsion System Module

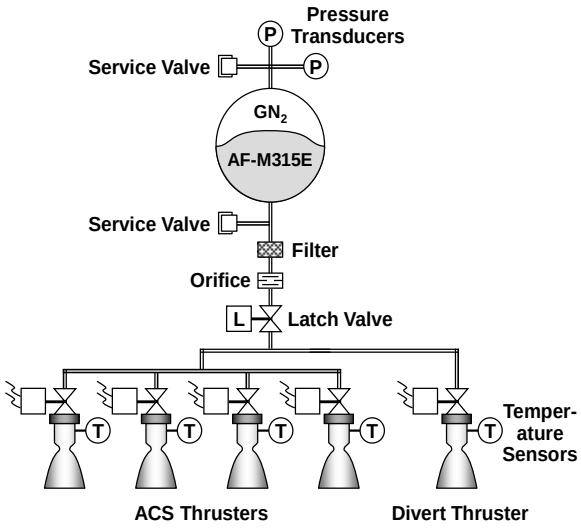

Figure 3: Propulsion System Schematic

GPIM GREEN ADVANCED MONOPROPELLANT THRUSTERS

Representing the culmination of over two decades of research and development, the GR-1 and GR-22 advanced monopropellant thrusters (Figure 4) combine a breakthrough high temperature catalyst with stability-enhancing design techniques to enable duty-cycle-unlimited operation on state-of-the-art green ionic liquid propellants while delivering substantially improved performance and reduced handling costs compared to conventional toxic monopropellants. Though bearing general resemblance to the series-assembled valve, injector, catalyst chamber, and nozzle of standard catalytic hydrazine thrusters of similar thrust class, the common core architecture of both designs incorporates a number of optimizations specific to the increased thermal management requirements of high-performance (and higher flame temperature) advanced monopropellants. Most immediately distinctive are the thrusters' two-piece extended stand-off structures. Serving to minimize heat soak-back to the mounting interface during and following extended thruster firings, this innovative design approach confines the need for high-temperature refractory alloys to the thrust chambers and nozzles, allowing a significant portion of both thrusters to be fabricated from lower cost-conventional nickel alloys. In supporting the thrust chamber from the downstream end, this increased thermal isolation is accomplished with no added length in either case, while heat dissipation during catalyst bed preheating to the nominal 315 ºC start temperature, and thereby associated power, are minimized.

Both thrusters also employ notably smaller, single-seat valves with higher net reliability than the two-seat scheme generally favored for comparable hydrazine thrusters. This results from an inadvertent benefit inherent to specific properties of ionic liquid propellants. Being typically more viscous than hydrazine, AF-M315E propellant is intrinsically far less prone to leakage, such that the added cost and doubled risk of a thruster becoming inoperable in the event of either of two redundant stages failing closed is not justified. Moreover, having essentially no vapor pressure, true ionic liquids will not self-pressurize or evaporate through small fissures such as a flaw in a valve seat. In the very unlikely event that thruster valve leakage should occur, isolation of the downstream feed system by closing an upstream system latch valve will fully prevent any loss of propellant. Likewise for launch range operations, the innate safety of ionic liquid propellants, accounting for both their low vapor toxicity and inability to activate un-preheated thrusters or react with external system and immediate work environment materials (unlike hydrazine), obviates conventional rationale for the use of dual-seat thruster valves. Thus, single seat valves provide higher mission assurance at lower mass, power (partially offsetting added preheat power requirements), and cost. Further, the resulting compactness of the GR-1 and GR-22 designs facilitates integration within the close packaging of small spacecraft where the high ρI_{sp} offered by ionic liquid propellants is most advantageous. Single seat valves have actually been used on many hydrazine-propelled spacecraft, and particularly NASA missions such as Cassini, Deep Impact, New Horizons, and Voyager (still successfully operating since its launch in 1977). Note, however, that unlike these examples, range safety has not required the addition of a secondary upstream latch valve to compensate for the loss of redundant leak inhibits on the thrusters for the GPIM demonstration, owed the inherent safety characteristics of the propellant.

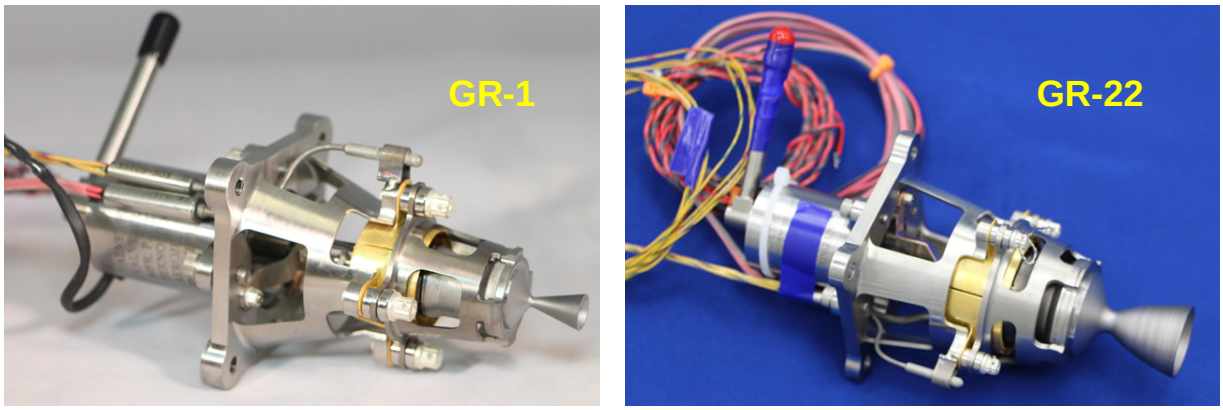

Figure 4: Prototype Aerojet GR-1 (left) and GR-22 (right) Thrusters

In accordance with engineering best practices, both thruster designs incorporate redundancy on all fracture-critical structural elements, including both portions of the mounting structures and all bolted joints/interfaces. Engineered to the same composite dynamic load specifications developed by Aerojet Rocketdyne to ensure broad mission utility for state-of-the-art hydrazine thrusters, the GR-1 and GR-22 are readily infusible into a wide range of applications where conventional monopropellants currently dominate.

PROTOTYPE THRUSTER TESTING

Testing of the GPIM prototype thrusters was conducted in the Aerojet Rocketdyne Advanced Propellants Test Lab (APTL) 1.8 m dia × 2.6 m long cylindrical stainless steel high-altitude chamber (see Figure 5) as equipped with a 64-channel Dewetron 204 kS/s data acquisition system and dual Stokes 1739 combination vacuum pumps. Because the refractory construction of the thruster chambers precludes practical direct attachment of a pressure tap, thruster performance and health were monitored via direct thrust measurement and a platinum-rhodium pitot probe directed into the plume on the nozzle centerline, as can be seen in the test set-up photos presented in Figure 6. Temperature instrumentation comprised a comprehensive array of type B and type K thermocouples affixed at various locations on the thrust chamber and supporting structure, catalyst bed heater, and control valve, as well as a Jenoptik VarioCAM thermal imaging camera. The test setup also included an argon purge ring, installed to direct a radial array of argon gas jets toward the thrusters whenever hot to minimize exposure of refractory metal surfaces to residual air in the chamber and plume backflow.

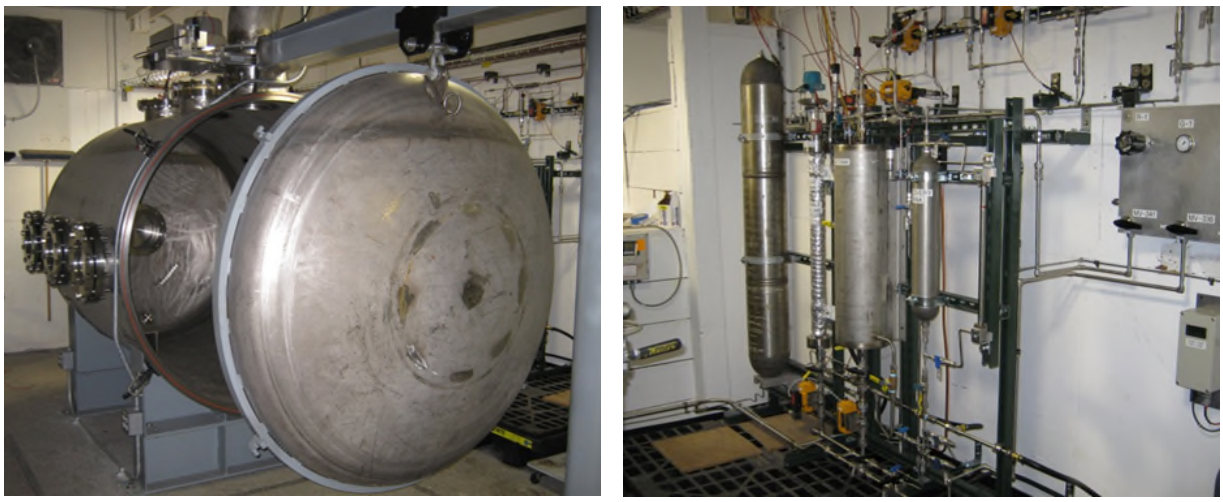

Figure 5: Advanced Propellants Test Lab High Altitude Cell (left) and Propellant Feed system (right)

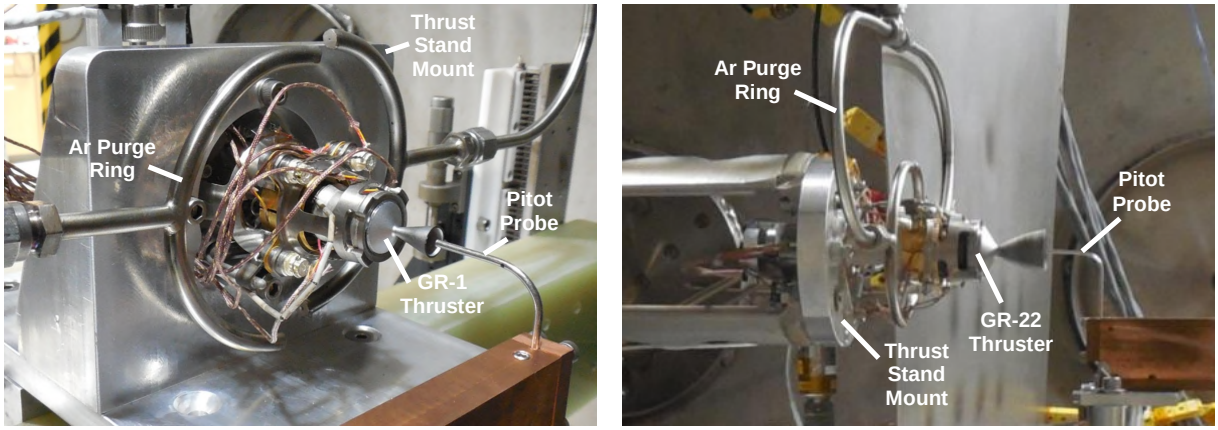

Figure 6: Prototype GR-1 (left) and GR-22 (right) Thrusters Installed in APTL Test Cell

Test operations, conducted 6/5-7/6/2014 and 8/21-10/8/2014 for the respective GR-1 and GR-22 thrusters, proceeded according to the following three sequential phases:

Phase 1: Extended Acceptance Test Procedure Hot-fire – Basic functional and stability verification as planned for flight unit acceptance testing, followed by performance mapping over a broad range of duty cycles.

Phase 2: Vibration Testing – Conducted on three spacecraft reference coordinate axis.

Phase 3: Protoflight Hot-Fire Test – Extended pulse-mode and steady-state performance characterization, followed by a life accumulation segment comprising alternating pulse-mode health-check and 20-min steady-state burns.

The GR-1 prototype was tested through approximately 3× planned demonstration mission life, corresponding to 4.47 kg total propellant throughput out of an estimated life capability of 12 kg (based on prior testing of functionally-equivalent heavyweight test units). Testing of the GR-22 prototype proceeded through Phases 1 and 2 without incident, but was terminated at approximately 3 kg accumulated propellant throughput (out of an estimated 15 kg total life capability) when a crack was detected in the thrust chamber. Both thrusters exhibited close-to-predicted thrust, I_{sp}, and start-up response characteristics, as well as high pulse-to-pulse repeatability. Key thruster functional characteristics and demonstrated performance are summarized in Table 1.

Table 1: GPIM Thruster Functional Characteristics and Demonstrated Performance Summary

	GR-1	GR-22
Nozzle Expansion Ratio:	100:1	100:1
Valve Power @ 28VDC, 10 ºC (W):	8.3	15.9
Feed Pressure (bar):	37.9-6.9	37.9-6.9
Thrust (N):	1.42-0.26	26.9-5.7
Maximum Steady-State I_{sp} (s):	231	248
Total Pulses:	11,107	944
Estimated Max Propellant Throughput Capability* (kg):	12	15
Prototype Test Propellant Throughput (kg):	4.47	3.0
Prototype Test Longest Burn (min):	20	1
Prototype Test Shortest Commanded Pulse Width (ms):	20	20

* Based on heavyweight thruster life testing conducted entirely at high thrust; longer life projected for thruster operated in blow-down mode.

GR-1 Prototype Test Performance

Normalized start-up transient thrust profiles for the prototype GR-1 (per direct measurement) vs. its heavyweight antecedent (as computed from thrust chamber measurements) are superimposed for comparison in Figure 7. The illustrated high degree of similarity demonstrated between the two test units confirms that the insulation scheme employed in the heavyweight unit provides sufficient thermal isolation of the thrust chamber such that heat dissipation to the walls is minimal, indicating all performance metrics previously established by heavyweight testing can be expected to carry forward for flight thrusters. Measured thrust and I_{sp} are plotted vs. feed pressure in Figure 8. Curve fits to the data suitable for use in

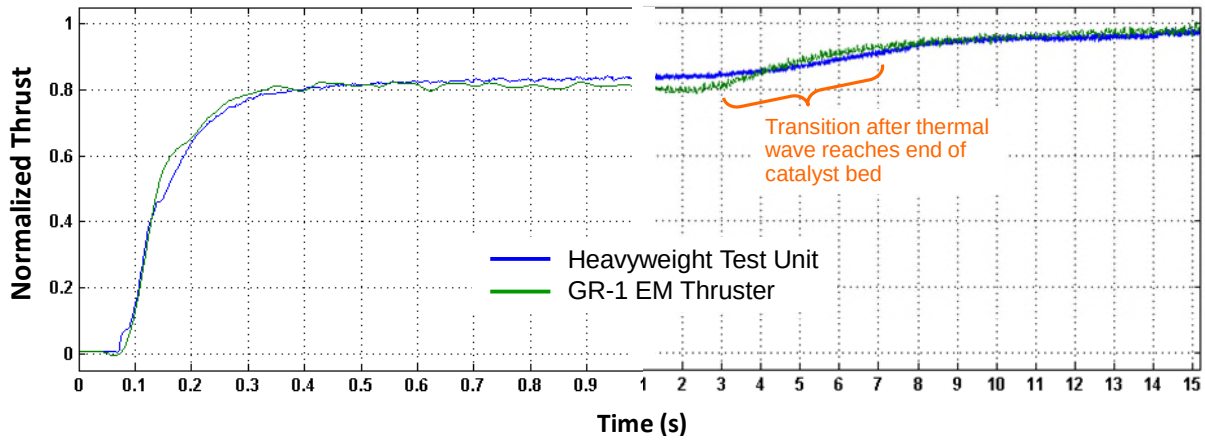

Figure 7: Comparison of Normalized Start-up Thrust Traces for GR-1 Prototype and Heavyweight Test Article

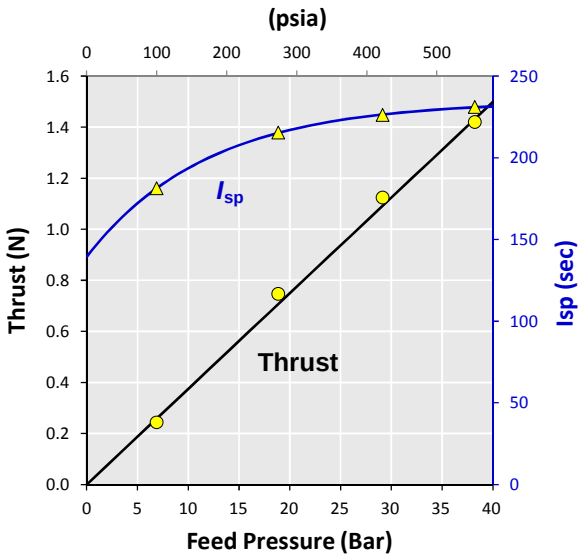

Figure 8: Prototype GR-1 Measured Thrust and I_{sp} vs. Feed Pressure

engineering performance predictions, also plotted in the figure, are provided as follows:

$$Thrust = [F/P]P_f \quad \text{where} \quad [F/P] = 0.037464 \ \text{N/bar}$$

$$Isp = Isp_o + (Isp_\infty - Isp_o)\left(1 - e^{-\frac{P_f - P_{ref}}{\Gamma}}\right)$$

$$\text{where} \begin{cases} Isp_o = 165.9 \ \text{sec} \\ Isp_\infty = 234.7 \ \text{sec} \\ P_{ref} = 3.878 \ \text{bar} \\ \Gamma = 11.90 \ \text{bar} \end{cases}$$

Pulse mode performance characterization for the GR-1 spanned a comprehensive range of duty cycles (ranging from 0.5% to 100%) and feed pressures (6.9, 19.0, 12.3, 29.3, and 37.9 bar). Throughout testing, thruster performance remained consistent with prior heavyweight development units, effectively confirming the broad operational utility necessary to serve as drop-in replacements for their hydrazine counterparts (in missions of appropriate duration). Figure 9 provides a comparison of pulse shape as measured by the pitot probe (taken at common feed pressure and pitot probe configuration), for an example set of duty cycles, where pulse order of execution is denoted by color gradation from blue for the first pulse, to red for the last.

Examples of two pulse trains, both executed at 29.5 bar (425 psia) feed pressure from the nominal preheat condition but varying in commanded on-time by an order of magnitude, are shown in Figure 10. Whereas the 200/178 ms on/off sequence is observed to vary continuously over twenty executed pulses, the 20/180 ms on/off sequence, corresponding to a lower terminal mean catalyst bed temperature, reaches cyclic thermal equilibrium relatively quickly, demonstrating a near-limit-cycle pulse-to-pulse impulse bit variability of <0.6% root-mean-square-standard deviation. Significantly better than typical of 1-N class hydrazine thrusters operating at similar duty cycles, the observed high pulse-to-pulse repeatability likely results largely from reduced valve hysteresis incurred as an inadvertent benefit of the propellant compatibility-necessitated titanium cladding of the thruster valve's ferromagnetics.

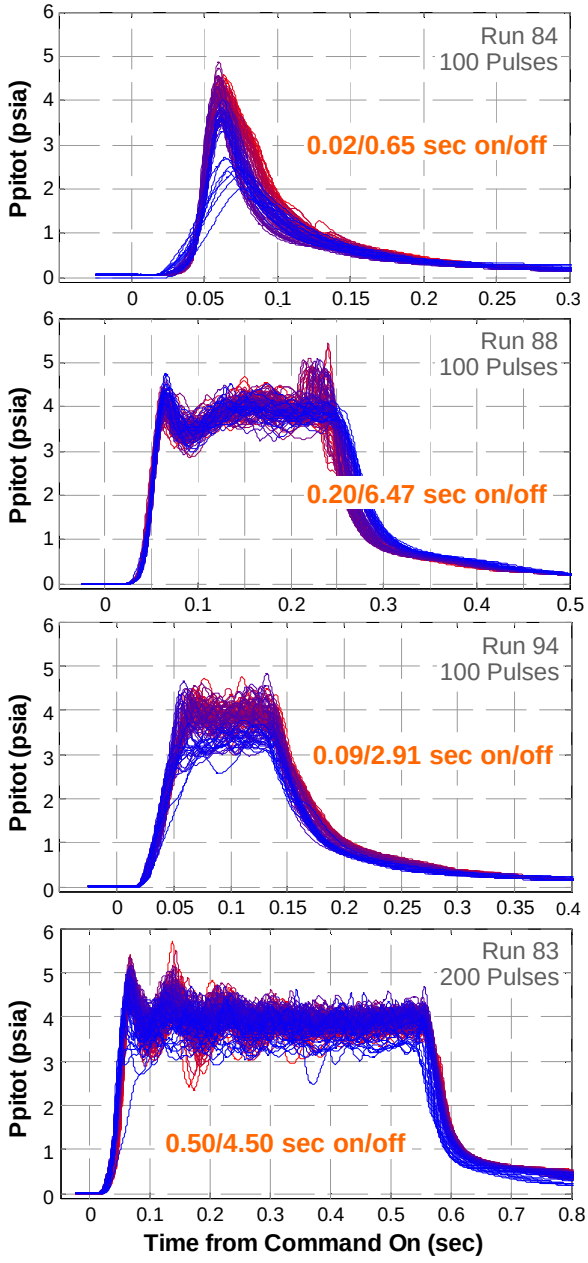

Figure 9: Pitot Probe Traces for Miscellaneous Duty cycles, Pf = 29.5 bar (425 psia)

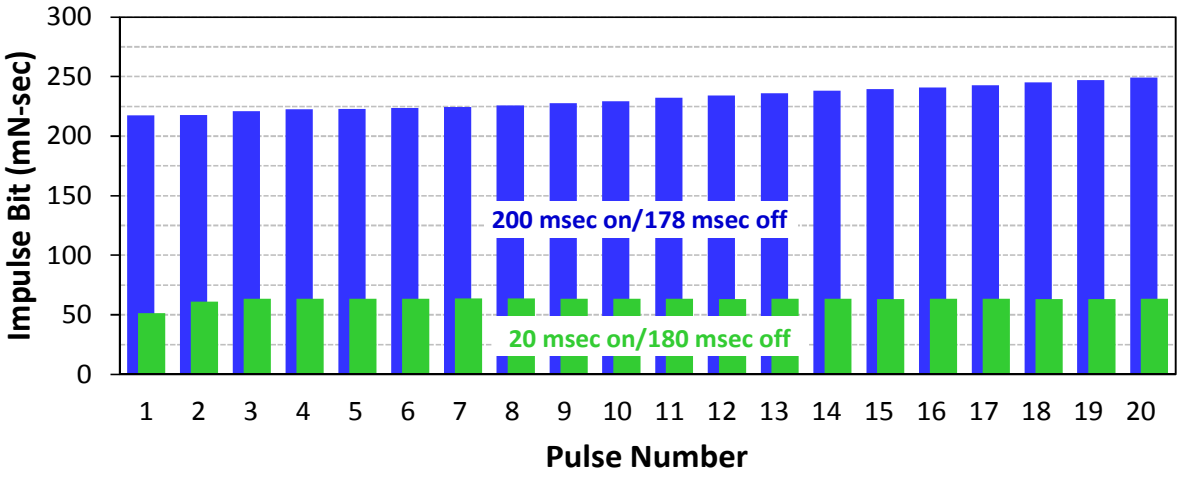

Figure 10: Ibit for 20 and 200 ms Pulse Sequences

Additional 435 psia feed pressure, 20/180 ms on/off pulse trains presented in Figure 11 provide an illustration of how Ibit and Ibit repeatability trended over thruster life. Disregarding differences in the first half of each sequence associated with dissimilar initial catalyst bed temperatures, a ~10% decline in Ibit, likely resulting from initially rapid increased flow pressure drop due to normal burn-in sintering/settling of the catalyst bed, was observed to occur early in firing life without substantial increase in pulse-to-pulse variability. A later sequence shows no progression of the earlier magnitude reduction, but the introduction of a small, qualitatively sinusoidal variation in Ibit as the catalyst ages, consistent with prior heavyweight test thruster performance. Both thrust stand and pitot probe-derived data showed pulse-to-pulse variability (computed as the running five-pulse root mean square standard deviation, excluding pulses near the beginning of each train affected by thermal transients as distinguished by initial monotonically increasing Ibit) for the large majority of pulses executed near the beginning of life to have been well below 1%, with isolated excursions up to ~5%; increasing to approximately 2% with isolated excursions to 10% by the end of the test.

GR-22 Prototype Test Performance

Prototype GR-22 start-up thrust and plume pitot probe recovery pressure traces are superimposed with chamber pressure data taken during prior representative heavyweight thruster testing in Figure 12. For

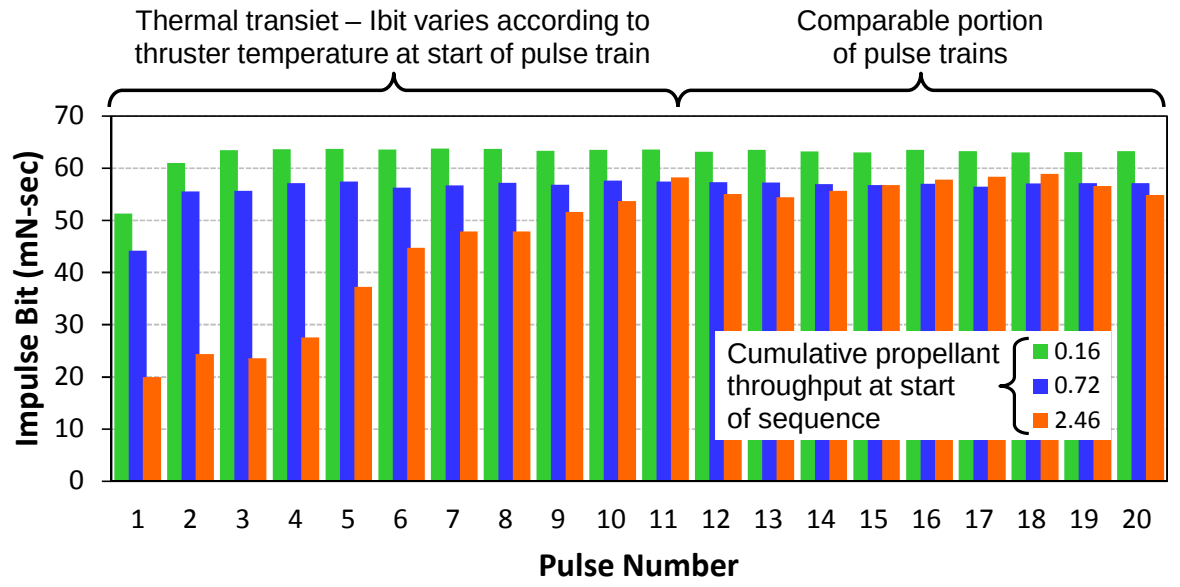

Figure 11: Variation in Ibit for 200/180 ms on/off Pulse Trains with Increasing Cumulative Propellant Throughput

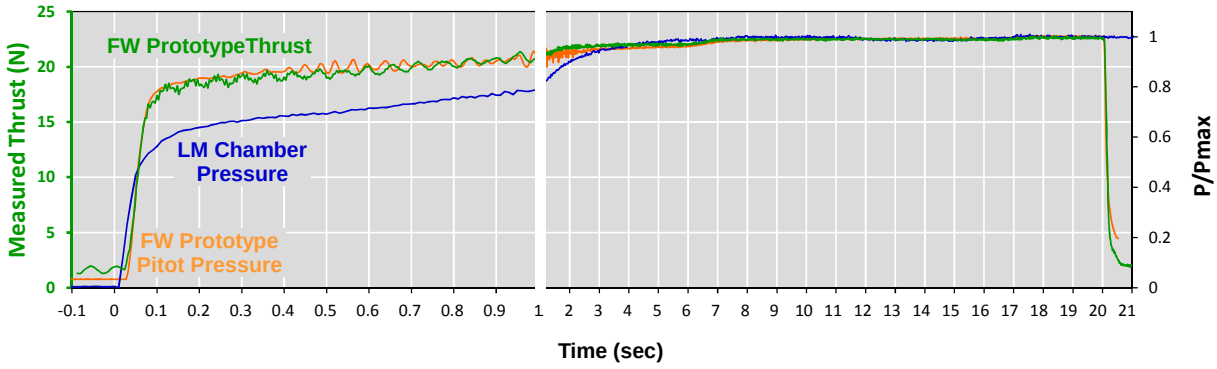

Figure 12: GR-22 Comparison of EM measured thrust and plume pitot probe pressure to LM chamber pressure

consistency, cases where the two thrusters were operated at similar thrust level and started from similar catalyst bed preheat temperature were selected for comparison. While remaining qualitatively similar, the two sets show greater differentiation than was observed for the 1-N thruster, suggesting greater relative differences in heat transfer characteristics between the two test units. Most readily notable is the rollover of the heavyweight thruster pressure trace from the initial rapid start-up transient at ~30% lower pressure, with the subsequent rise evidencing a heat-up time-constant approximately two times that of the flight-weight prototype.

Although testing or the GR-22 prototype test was stopped prematurely due to the formation of a crack in the rhenium chamber wall, all baseline performance characterization test sequences were completed. Measured thrust and I_{sp} are plotted vs. feed pressure in Figure 13 alongside curve fits, expressed for use in engineering performance predictions as follows:

$$Thrust = [F/P]P_f\left(1+\frac{\Gamma}{P_o+P_f}\right)$$

$$\text{where } \begin{cases} [F/P] = 0.077416 \text{ N/bar} \\ \Gamma = 1594 \text{ bar} \\ P_o = 157.1 \text{ bar} \end{cases}$$

$$Isp = Isp_o + \left(Isp_\infty - Isp_o\right)\left(1 - e^{-\frac{P_f - P_{ref}}{\Gamma}}\right)$$

$$\text{where } \begin{cases} Isp_o = 222.1 \text{ sec} \\ Isp_\infty = 249.3 \text{ sec} \\ P_{ref} = 1.113 \text{ bar} \\ \Gamma = 10.95 \text{ bar} \end{cases}$$

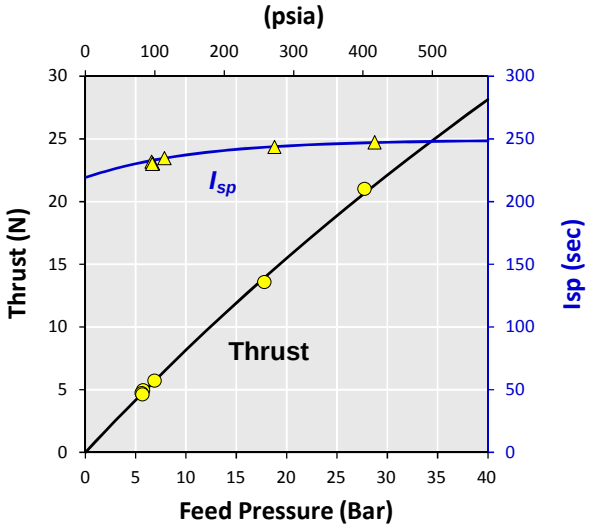

Figure 13: Prototype GR-22 Measured Thrust and I_{sp} vs. Feed Pressure

Vibration Testing

Random vibration testing was performed sequentially along orthogonal X, Y, Z axes as defined according the thrusters' alignments in the spacecraft coordinate plane. Note that while the as-installed GR-22 axis of symmetry is aligned with the spacecraft X-axis, such is not the case for the GR-1 thrusters, which are mounted (and were therefore tested) at skew angles. Tested levels for both prototype thrusters, presented in Figure 14, were 3dB above maximum mission projected envelope (MPE) with the exception of along the Y and Z axes for the GR-1, instead tested at MPE due to an interfering test fixture resonance (subsequently resolved in preparation for acceptance testing of flight units). It should be noted that the tested levels, while sufficient to meet demonstration mission needs, are conservative with respect to thruster actual MPE+6dB design

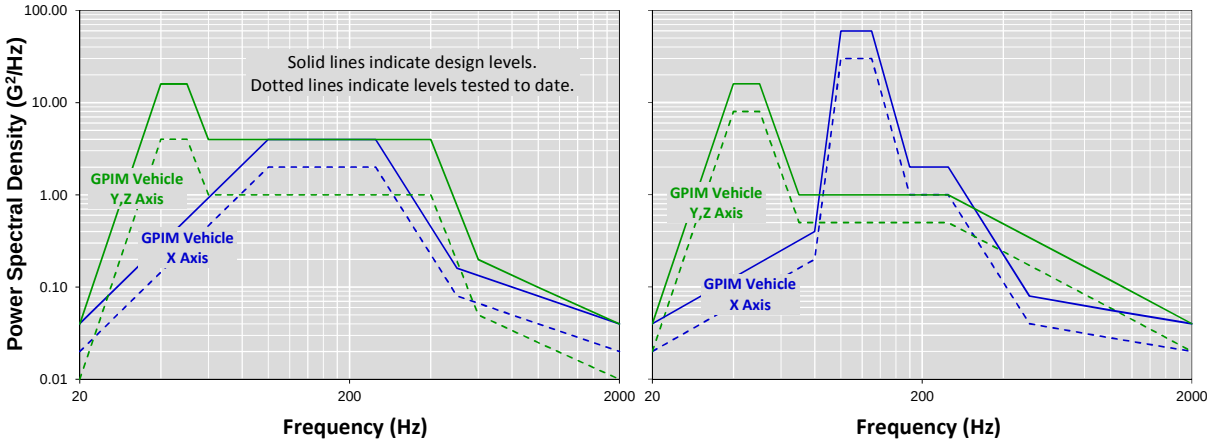

Figure 14: GR-1 (Left) and GR-22 (Right) Design vs. Prototype Vibration Test Power Spectra

capabilities, also depicted in the figure. Both thrusters completed testing with no observable shift in fundamental frequencies. Likewise, no defects were detected in post-test inspection.

CONCLUSION

The combined high impulse density and inherent handling simplicity of advanced green monopropellants such as AF-M315E are particularly advantageous for smallsats. As such, it is no coincidence that the first on-orbit demonstration of an AF-M315E propulsion system, the capstone of NASA's four-year GPIM program, will be aboard an ESPA-class spacecraft. With respect specifically to the engineering of smallsat systems, the GPIM program represents more than a demonstration, but validation of a flight-proven, high-performance (50% greater ρI_{sp} than hydrazine) complete propulsion solution, ready for deployment on future missions. Intended to bracket the broadest range of thrust levels applicable to smallsats, both 1-N and 20-N class thrusters have respectively been developed to flight-ready and near-flight-ready states. Because an additional test iteration will be necessary to fully retire flight risk for the 20-N class GR-22 thruster, but cannot be concluded within the remaining time available, the GPIM demonstration will continue on the present schedule using exclusively 1-N class GR-1 thrusters. In parallel, already-complete design updates to the GR-22 will be verified by test later in 2015, when the APTL facility becomes available following completion of ongoing hot-fire acceptance testing of the GPIM flight hardware. The GPIM propulsion module (shown partially assembled in Figure 15) is slated for delivery for integration with the spacecraft bus in late August 2015 and subsequent launch as a secondary payload aboard the second flight of the Falcon Heavy launch vehicle in 2016.

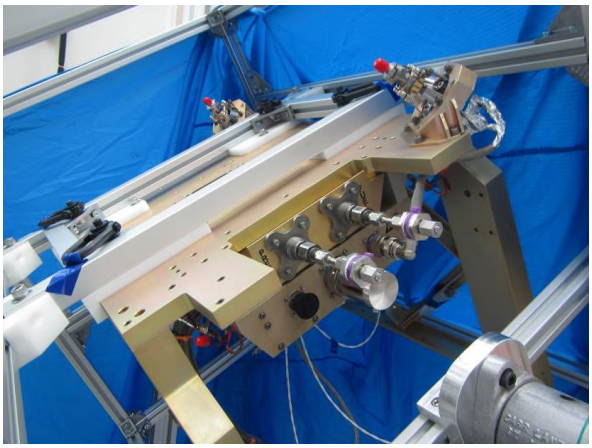

Figure 15: In-Work GPIM Demonstration AF-M315E Propulsion Module on Handling Fixture

ACKNOWLEDGMENTS

The authors wish to thank the NASA Space Technology Mission Directorate Technology Demonstration Mission (TDM) office for funding the GPIM technology demonstration program, NASA Glenn Research Center for their plume modeling efforts on the GPIM program and loan of data acquisition equipment, NASA Goddard Space Flight Center for their work in characterizing propellant water hammer properties, and the AFRL for their participation in the GPIM program to develop ground support equipment, experimental characterization of propellant surge properties, and loan of/assistance with the high precision, high response thrust stand employed in testing of the GR-1 prototype and flight thrusters.

References

1. McLean, C., Spores, R., Sheehy, J., "Green Propulsion Infusion Mission, Program Construct, and Mission Objectives", Commercial and Government Responsive Access to Space Technology Exchange (CRASTE) Conference, Bellevue, WA, 24-27 June, 2013.
2. McLean, C., Spores, R., Sheehy, J., "Green Propulsion Infusion Mission, Program Construct, and Mission Objectives", 60th JANNAF Propulsion Meeting, Colorado Springs, CO, May 2013.
3. Mclean, C.H, Hale, M.J., Deininger, W. D., Spores, R.A., Frate, D.T., Johnson, W.L., Sheehy, J.A, " Green Propellant Infusion Mission Program Overview", 49th AIAA/ASME/SAE/ASEE Joint Propulsion Conference, San Jose, CA, July 2013.
4. Deininger, W., et al, "Implementation of the Green Propellant Infusion Mission (GPIM) on a Ball Aerospace BCP-100 Spacecraft Bus", 49th AIAA/ASME/SAE/ASEE Joint Propulsion Conference, San Jose, CA, July 2013.
5. Yim, J.T., Reed, B.D., Deans, M.C., McLean C.H., Sheehy, J.A., "Green Propellant Infusion Mission Plume Impingement Analysis", 49th AIAA/ASME/SAE/ASEE Joint Propulsion Conference, San Jose, CA, July 2013.
6. Spores, R.A, Masse, R.K., Kimbrel, S, Spores, R.A., Mclean, C.H., " GPIM AF-M315E Propulsion System Development", 50th AIAA/ASME/SAE/ASEE Joint Propulsion Conference, Cleveland, OH, July 2014.
7. Sackheim, R.L., Masse, R.K. "Green Propulsion Advancement: Challenging the Maturity of Monopropellant Hydrazine", Journal of Propulsion and Power, Vol. 30, No. 2 (2014), pp. 265-276.
8. Personal communication with Eric Cardiff, NASA Goddard Flight Center.
9. Meinhardt, D., Wucherer, E., Brewster, G., "HAN-Based Monopropellant Vehicle ACS Trade Study," Primex Aerospace Document R-97-2105, prepared for the NASA Lewis Research Center Launch Vehicle Project Office, September 1997.